Polymer encapsulation effects on the magnetism of EuS nanocrystals†

Angela Sofia Pereira,[a] Protima Rauwel,[a] Mário Souza Reis,[b] Nuno João Oliveira Silva,[c] Ana Barros-Timmons[a] and Tito Trindade*[a]

Received 16th April 2008, Accepted 30th June 2008
First published as an Advance Article on the web 20th August 2008
DOI: 10.1039/b806499g

Surface mediated phenomena are important in controlling the magnetism of nanocrystals. Here, we provide a versatile chemical method which allows the formation of EuS nanocrystals encapsulated in poly(styrene) (PS). These materials are the first example of a polymer based EuS nanocomposite prepared *in situ*. Besides their practical interest, these materials are of general relevance because they allow fundamental knowledge on the magnetism of EuS, which is commonly used as a model of an insulating ferromagnet, to be acquired. Comparatively to the starting powders of EuS nanocrystals (8 nm), in the final nanocomposites there is a decrease of the blocking temperature T_B and a change in the shape of the field-cooled susceptibility curve, indicating that the intensity of dipolar interactions decreases when the nanoparticles are incorporated into PS. Differences in the magnetic properties of the EuS nanocrystals and the EuS/PS nanocomposites are also due to the appearance of a peak in the susceptibility at 60 K, in the latter sample, ascribed to surface phenomena occurring in EuS nanocrystals dispersed in the polymer matrix.

Introduction

Nanocrystals have drawn a large amount of attention due to the enormous variety of physical properties given by the size tuning of these materials, which differ from their bulk counterparts.[1] Over the past decade, a range of wet chemical methods for the preparation of nanoparticles have been employed, including the most commonly used procedures based on chemical reactions of molecular precursors in high boiling point solvents.[1,2] A variant of these methodologies makes use of single-molecule precursors for the preparation of several semiconductor nanocrystals.[3] The relevance of this approach has been recently confirmed for the case of EuS, for which europium (III) alkyldithiocarbamates were used as single-sources to prepare high quality EuS nanomaterials.[4–7]

Europium mono-chalcogenides (EuE, E = O, S, Se, Te) with the rock-salt structure have been investigated at least since the 1960s.[8] The europium chalcogenides form an important class of magnetic semiconductors, revealing an assortment of magnetic ordering,[8] and have frequently served as model Heisenberg magnets.[9,10] Research on the effect of particle size and surface nature on the magnetic properties of the europium chalcogenides has become very appealing; for example, pressure studies have shown that the Curie temperature (T_C) is very sensitive to both the Eu–Eu distance and the band gap energy.[11] Among the europium mono-chalcogenides, EuS has been especially investigated due to its properties as a ferromagnetic semiconductor with a Curie temperature of 16.8 K, an energy gap of 1.6 eV, and a spin-splitting of the gap of 0.36 eV. Lately, nanocrystalline EuS has established its potential as an optomagnetic material.[12,13] This is a promising material as a component for the manufacture of devices that can be tuned by material responses to magnetic, electrical, and optical stimuli. This suggests possible optoelectronic applications for EuS nanocrystals in optical isolators, optical circulators, and optical memory.

At present, there is a range of synthetic methods that gives us the ability to prepare high quality inorganic nanoparticles, thus these materials have been recently explored as nanoscopic fillers in polymer matrices in the advancement of functional nanocomposites.[14,15] In this regard, a number of polymer nanocomposite particles have been prepared through a variety of chemical methods which include heterophase polymerization,[16] heterocoagulation,[17] and layer-by-layer self-assembly.[18] Heterophase polymerization is by far the most frequently used technique to obtain nanocomposite particles. These can be prepared by carrying out the polymerization *in situ* in the presence of the inorganic nanofillers or their precursors.[19] Among these methods, miniemulsion polymerization has established itself as an important synthetic strategy to obtain nanocomposites of diverse materials, including glasses, semiconductors, metals and carbon nanotubes as nanofillers.[20] In miniemulsion polymerization, particle nucleation takes place, for the most part, within nanometre monomer droplets.[20] In view of the fact that organically capped inorganic particles can be dispersed in the monomer after miniemulsification, then each miniemulsion droplet acts as a true nanoreactor. Some characteristics of the miniemulsion polymerization system offer prospective advantages for the encapsulation of nanoparticles, specifically, the capability to

[a]*Department of Chemistry and CICECO, University of Aveiro, 3810-193 Aveiro, Portugal. E-mail: tito@ua.pt; Fax: +351 234370084; Tel: +351 234370360*
[b]*Department of Physics and CICECO, University of Aveiro, 3810-193 Aveiro, Portugal*
[c]*Instituto de Ciencia de Materiales de Aragón, Universidad de Zaragoza-CSIC, Departamento de Fisica de la Materia Condensada, Faclutad de Ciencias, 50009 Zaragoza, Spain*

† Electronic supplementary information (ESI) available: Powder XRD of EuS and EuS–PS samples; FT-IR spectra for both EuS–OA nanocrystals and their poly(styrene) derivative nanocomposites; TEM image of a nanocomposite sample obtained using EuS nanocubes; histograms of the EuS nanospheres. See DOI: 10.1039/b806499g

nucleate all the droplets containing the inorganic nanoparticles, good control of droplet size and size distribution, and direct dispersion of the nanoparticles within the organic phase.

In the past two decades, considerable research on semiconductor nanocrystals has clearly demonstrated that these particulates show unique size-dependent properties. Along this line of research, the way the collective properties developed from individual nanocrystals to their assemblies have emerged as a less understood issue in solid state science. In this respect, nanocrystals that tend to self-organize into more complex nanostructures are interesting systems of study and this seems to be the case for nanosized EuS.[4–6,21] We adopted here a new approach to fabricate assemblies of EuS nanocrystals by promoting their encapsulation in a polymer matrix. Our aim in this study was to investigate the effects of the polymer encapsulation on the magnetic properties of EuS nanocrystals; this is clearly appealing from the academic point of view, in particular when considering that EuS is a common model of a Heisenberg magnet. In addition, by combining EuS nanocrystals with polymers, the resulting material can find further interest for the emerging field of polymer nanodevices. To date this is the first report of the *in situ* synthesis and magnetic behaviour of morphological well-defined EuS/polymer nanocomposites.

Results and discussion

Nanocrystals synthesis and structural characterization

The thermal decomposition of single-molecule precursors has proven to be a valuable method for synthesizing nanosized metal chalcogenides.[3] Coordinating solvents, such as oleic acid, alkylphosphine oxides, hexadecylamine or oleylamine, have been used as the reacting media which also allows further colloidal stabilization by capping the nanocrystals' surfaces during the synthesis.[22] In this work, and as a first approach to the synthesis of EuS/polymer nanocomposites, the synthesis of EuS nanocrystals was performed using oleylamine, acting mutually as the reacting solvent and the stabilizer.

Fig. 1 shows the TEM images of synthetic EuS/OA nanocrystals which have been used in this work as the starting materials to prepare the polymer nanocomposites. Two types of morphology were observed for the EuS nanocrystals and which one is seen depends on the synthesis conditions. Nearly monodisperse EuS nanospheres ($d \approx 8$ nm) were obtained when injecting the single-molecule precursor into hot OA while larger EuS nanocubes were prepared by heating the precursor together with the solvent. Assessment of the XRD patterns of EuS/OA nanocrystals revealed the expected rock-salt type crystal structure with all the Bragg reflections indexed to pure EuS (ESI†). This result was further confirmed by selected area electron diffraction (SAED) performed on diverse nanosized EuS samples. The average size of the nanospheres was estimated to be 8 nm by applying the Scherrer equation to the XRD results, which is in fair agreement with TEM analysis.

The assumption that OA is coordinating the EuS nanocrystals' surfaces is based on the observed hydrophobic characteristics of these particulates, which can be explained because the hydrocarbon chains of OA molecules are directed outwards. As will be described in the next section, these hydrophobic nanocrystals can

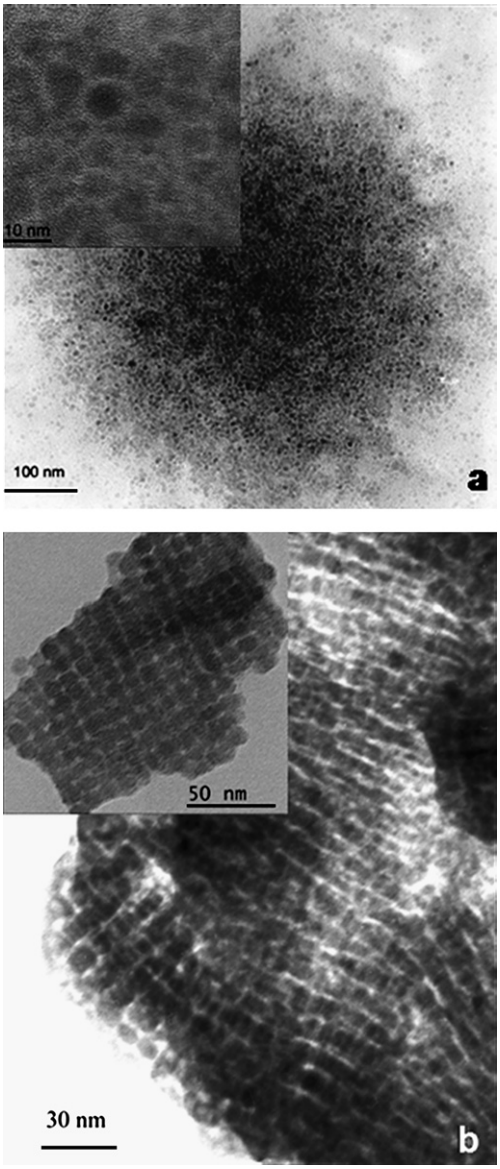

Fig. 1 TEM images of oleylamine capped EuS nanospheres (a) and nanocubes (b).

be easily dispersed in an organic medium, such as the monomer styrene, to perform *in situ* polymerizations. Confirmation of the presence of OA molecules at the EuS nanocrystals' surfaces was obtained by means of FT-IR spectroscopy performed on a sample previously washed with a mixture of isopropanol and methanol. The FT-IR spectrum clearly shows (ESI†) diagnostic bands from oleylamine: 3220, 3119 cm^{-1} (ν_{N-H}); 2919, 2849 cm^{-1} (ν_{C-H}); 1466 cm^{-1} (ν_{C-N}).

Polymer encapsulation of organically capped EuS nanocrystals

The EuS polymer nanocomposites were prepared by miniemulsion polymerization of styrene in the presence of the EuS/OA nanocrystals. As a first step, a stable aqueous miniemulsion was prepared by dispersing the hydrophobe (HD) and the EuS/OA nanocrystals in the styrene droplets. This organic phase was then dispersed in an aqueous solution of surfactant (SDS) and

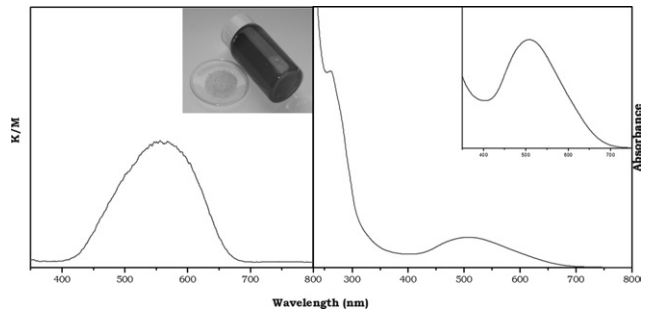

Fig. 2 Visible reflectance spectrum of a EuS/PS nanocomposite sample (left); inset shows a micrograph of the as prepared sample, both as a powder and as an aqueous emulsion. UV/VIS spectrum of the original EuS nanocrystals dispersed in toluene (right).

sheered using an ultrasound probe. The polymerization was then carried out under conventional free radical conditions using AIBN or KPS as the initiators and under a N_2 flow. A first evidence for the presence of EuS/OA nanocrystals in the final nanocomposite is the band centered at ~550 nm in the visible reflectance spectrum of the solid EuS/PS nanocomposite (Fig. 2). Compared to the original EuS nanocrystals (Fig. 2) this band is wider but still related to the electronic transition $4f^7(^8S_{7/2}) \rightarrow {}^4f^6(^7F_J)5d(t_{2g})^1$ occurring in Eu^{2+} ions.[4,6] It is this absorption band in the visible region that explains the purple color observed for the EuS/PS emulsion.

To prepare the nanocomposites, various parameters have been adjusted to achieve optimal reaction conditions (see Experimental methods section), namely in connection with the type of initiator and the concentration of surfactant. Depending on the experimental conditions, the chemical composition and the particle morphology of the nanocomposite was substantially altered. For example, when KPS was used as the initiator, the EuS nanocrystals invariably dissolved, resulting in loss of color and the final material turned into a film composed of large rice-shaped (12 μm) microparticles (Fig. 3a). This result, combined with those from EDS (energy dispersion spectroscopy), indicate that this sample contains mainly Eu and hardly any S; this suggests that persulfate radicals may be involved in the oxidation of the EuS nanocrystals. However, using AIBN as the initiator, colloidal stable emulsions could be prepared though two distinct particle size populations were observed. As suggested by TEM analysis (Fig. 3b), these two populations correspond to free PS particles and to EuS/PS nanocomposite particles, respectively. Successive centrifugation cycles yielded fractions which became subsequently richer in nanocomposite particles as compared to the starting emulsions. The remaining free polymer particles were analysed by GPC giving a molecular weight of 98 500 Da as compared to 154 000 Da, obtained for poly(styrene) prepared using similar conditions but in the absence of EuS nanocrystals. This lower molar mass is thought to be due to chain termination reactions of the growing polymer chains at the surface of the EuS nanocrystals.

It appears from our results that, in maintaining the same conditions of polymerization, the EuS particles morphology influences the polymer nanocomposite properties. Thus the EuS nanospheres tend to be encapsulated by poly(styrene) yielding round shaped nanocomposite particles, which can be present either as isolated nanocomposite particles (Fig. 4a) or clustered into raspberry-like particles (Fig. 4b). The latter morphology presumably results from the clustering of original EuS/PS nanoparticles and was the most common morphology observed in these nanocomposites. When considering the larger and cubic EuS nanocrystals (Fig. 1), and for similar conditions of miniemulsion polymerization, we could not obtain the polymer encapsulation of the nanoparticles. Instead, TEM analysis showed that the EuS nanophase remained mainly outside the polymer beads (ESI†). This is probably due to the larger size of the nanoparticles (or their assemblies) compared to the monomer droplet dimensions in the reacting system.

These observations indicate that ensembles of EuS nanospheres can be coated with poly(styrene) and this might induce changes in the magnetic behaviour of EuS. Therefore, we have decided to focus our attention on the nanocomposites containing the EuS nanospheres ($d \approx 8$ nm) and to investigate in detail the magnetism of a selected nanocomposite sample with 5% (w/w) in relation to the Eu content, as determined by ICP analysis. Although we did not find vestiges of europium oxides in the powder XRD of the nanocomposite (ESI†), the oxidation of the EuS surfaces cannot be ruled out, as will be discussed below.

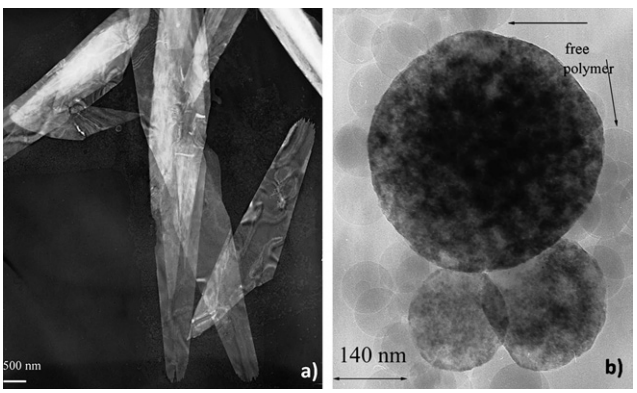

Fig. 3 TEM images of samples obtained after polymerization of styrene in the presence of EuS nanocrystals, using KPS (a) and AIBN (b) as initiators.

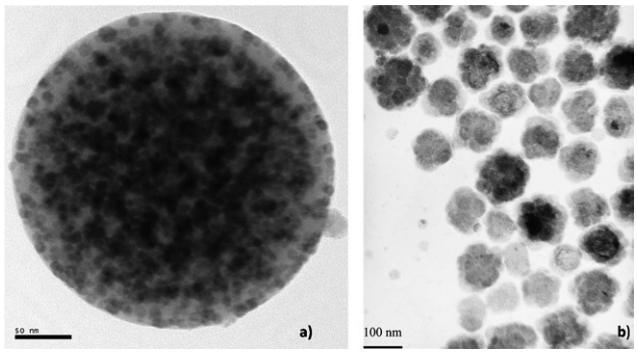

Fig. 4 TEM images of EuS/PS nanocomposite particles: (a) detail of a single spherical particle; (b) set of particles with raspberry-like morphology.

Magnetism of EuS/OA nanocrystals *vs.* magnetism of EuS/PS nanocomposites

In order to investigate the changes on the EuS magnetic properties when going from EuS/OA nanopowders to the respective EuS/PS nanocomposites, the former sample was first analysed, though relevant data on this parent system can also be found in the literature.[6,7]

The DC susceptibility curves of the EuS nanocrystals show a transition temperature T_C at around 15 K (estimated from the inflection point of the curves) and a thermal irreversibility below $T_{ir} = 14$ K. The zero-field-cooled (ZFC) curve has a maximum (blocking temperature) at $T_B = 7.7$ K. This T_B is higher than that found for 8 nm diameter nanocrystals (~5 K).[7] This may be due to a different intensity of dipolar interactions and/or different nanoparticle anisotropy. The field-cooled (FC) curve tends to saturate at low temperatures, as is usually found in bulk and interacting-nanoparticle systems.[23] An inspection of the temperature dependence of the inverse of the magnetic susceptibility shows that above T_C the system has two Curie–Weiss regimes: one above ~50 K with an extrapolated paramagnetic Curie temperature θ_p of 10.8 K, and other below ~50 K with an extrapolated θ_p of 15.7 K. This behaviour is depicted in Fig. 5(a). The ac susceptibility curves show a high temperature region (above $T_F \approx 15$ K), in which the in-phase susceptibility χ' is not frequency dependent and the out-of-phase susceptibility χ'' is close to zero. The $\chi'(T)$ curve exhibits a maximum at the blocking temperature T_B', which is frequency dependent. In addition, $\chi''(T)$ has a frequency dependent maximum T_B'' at around 5 K and a shoulder around 10 K. The existence of dynamics in the studied frequency range places the EuS in the context of nanoparticles/spin-glasses and not in the context of bulk materials.

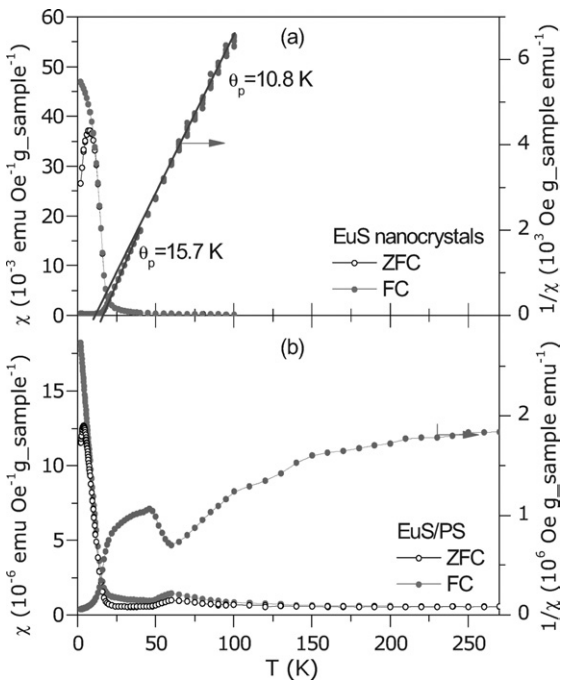

Fig. 5 DC magnetic susceptibility as a function of temperature, obtained from the ZFC and FC procedures: (a) EuS nanocrystals and (b) EuS/PS nanocomposites.

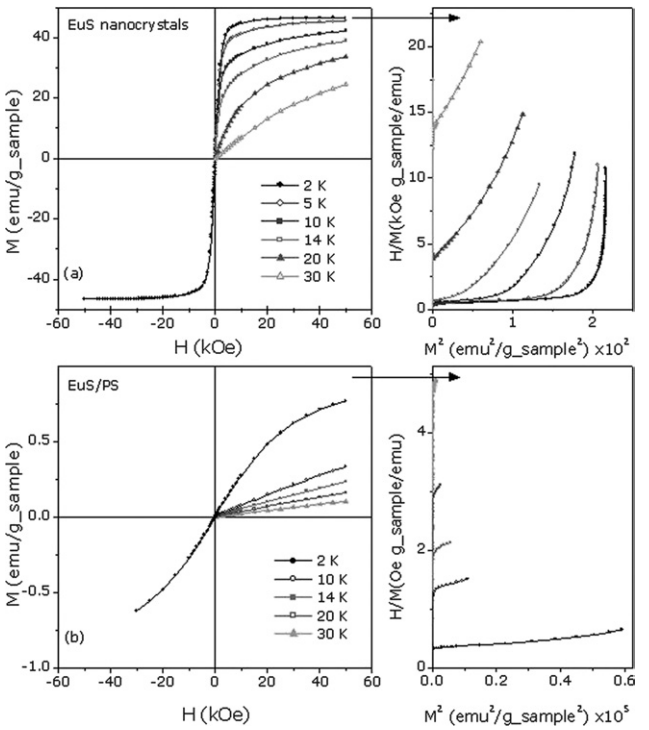

Fig. 6 Magnetization as a function of magnetic field for several temperatures for (a, left) EuS nanospheres and (b, left) EuS nanospheres embedded in poly(styrene). The corresponding Arrot plots are presented in the right-hand panels.

Details on the magnetization data as a function of magnetic field can be found in Fig. 6a, left. The EuS nanocrystals have low coercive fields H_C (at 2 K, $H_C = 90$ Oe) and low remanence M_r, this rapidly approaches zero as temperature increases, being zero above T_C (Fig. 7). We note that the M_r values were obtained after taking into account the contribution of the remanent field of the superconducting coil.[24] If this contribution is ignored, a spurious M_r with negative values for $T > 7$ K arises (Fig. 7). We remark that this spurious M_r is similar to that found in the literature.[25] Therefore, the EuS nanocrystals do not have

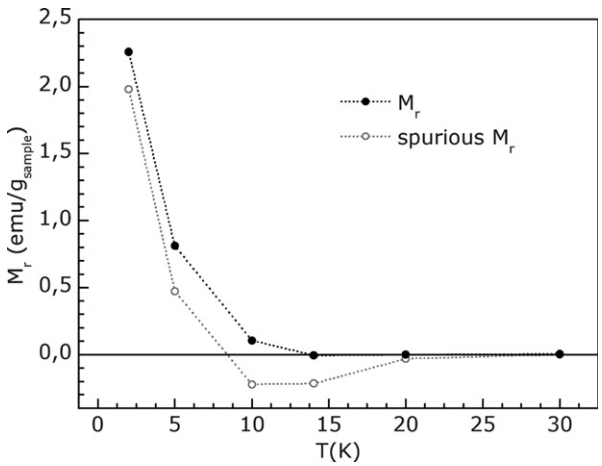

Fig. 7 Remanent magnetization as a function of temperature in EuS nanocrystals.

a magnetization reversal but a canonical behaviour of M_r decrease towards zero as T approaches T_C and a zero M_r for $T > T_C$. The Arrot plots shown in Fig. 6a, right, and obtained from the $M(H)$ curves, confirm that the Curie temperature is around 15 K. The gap between the measurement at 2 K and the M^2 axis is directly proportional to the demagnetization factor of the sample.

The DC susceptibility curves of EuS/PS nanocomposite show irreversibility up to a higher temperature than that of EuS nanocrystals (Fig. 5). Characteristic features appear in the (a) 2–20 K and (b) 40–100 K temperature ranges. For that first range, it is possible to observe an increase of the thermal irreversibility below ~7 K. In particular, the FC curve has no signs of saturation at low temperatures (paramagnetic-like curve), while the ZFC curve has a maximum at $T_B = 3.9$ K. In what concerns the other range (>40 K), we observe a maximum at 60 K (Fig. 6b), probably related to a EuO-like environment located at the surface of the nanocrystals, since EuO has a T_c at 69 K.[8] The AC susceptibility curves show a high temperature region $T_{ir} > 11$ K for which the in-phase susceptibility χ' is not frequency dependent and the out-of-phase susceptibility χ'' is close to zero. $\chi'(T)$ exhibits a frequency dependent maximum at around $T_B' = 4$ K. On the other hand, $\chi''(T)$ has a monotonic decrease to zero as the temperature increases up to 11 K. As shown in Fig. 6b, left, the magnetization as a function of magnetic field for the EuS/PS nanocomposite presents a quite different behaviour to that found for the EuS nanocrystals, which is probably related to an antiferromagnetic arrangement. Also shown in Fig. 6b, right are the Arrot plots for the nanocomposite, that confirm our previous findings based on the DC magnetic susceptibility measurements, that for this material no Curie temperature associated with EuS order is detected.

A comparative analysis of Fig. 5–7, clearly shows that the magnetic properties of the EuS nanocrystals change upon their incorporation into PS. In particular, we note that T_B decreases from 7.7 K to 3.9 K. The decrease of T_B and the change in the shape of the FC curve indicate that the intensity of dipolar interactions decreases when the nanocrystals are incorporated into PS.[26] Therefore, the average interparticle distance increases with their incorporation into PS, pointing out that the nanocrystals are efficiently dispersed in the PS media. Differences in the magnetic properties of the EuS and EuS/PS systems are also due to the appearance of a peak at 60 K. This is ascribed to surface phenomena, namely the existence of an oxidised surface in the EuS nanocrystals of the latter sample, as a result of the reaction conditions employed to synthesize the nanocomposites. The importance of the surface on the magnetic behaviour of EuS nanocrystals has also been recently observed for EuS prepared by a different route which involved the chemical reaction of Eu metal and H_2S in liquid ammonia.[27]

The effect of the polymer encapsulation on the dipolar interactions in nanosized EuS, was further confirmed by analysing the dependence of T_B' with the frequency of the AC field. In this regards, the Néel model applied to superparamagnetism predicts that the dependency of $\tau = 1/f$ with T_B' is described by:[28]

$$\tau = \tau_0 \exp\left(\frac{E}{k_B T_B'}\right) \quad (1)$$

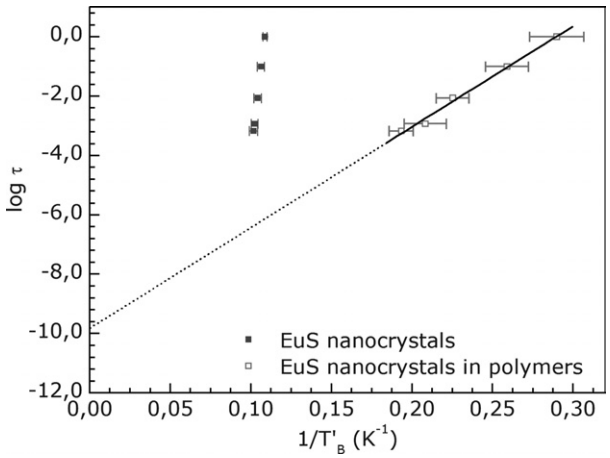

Fig. 8 Thermal variation of the relaxation time ($\log\tau$ *vs.* $1/T_B'$) by linearization of eqn 1 (see text for details).

where τ_0 is a characteristic microscopic time, usually in the 1×10^{-9}–10^{-17} s range. At low temperature, the particles cannot cross the energy barrier E to reverse the magnetization within the characteristic time of measurement τ. As the temperature increases, particles with lower energies start to cross the barrier, until $T = T_{ir}$ where all the particles can follow the field. E is usually expressed as the product of an effective anisotropy constant K_{eff} and the particle volume V. Thus, the thermal variation of τ of the EuS nanocrystals dispersed in PS is well described by eqn (1) with $E = 78(4)$ K and $\tau_0 = 2 \times 10^{-10}$ s (Fig. 8). Considering spherical nanoparticles with 8 nm of average diameter, $K_{eff} = 4(2) \times 10^4$ erg cm^{-3}. This is about one order of magnitude higher than that found in the literature.[19a] An enhancement of K_{eff} is usually associated with an increase in the surface anisotropy and spin disorder. The use of eqn (1) to describe $T_B'(\tau)$ in the EuS nanocrystals implies a too low τ_0 (1×10^{-49} s), without physical meaning, that excludes the description of the EuS nanocrystals as non-interacting entities. Noteworthy is the decrease of the extrapolated τ that is followed by an increase in E, as is usually found when dipolar interactions increase.[26,29] Therefore the EuS nanocrystals embedded in PS beads are well described by the superparamagnetic Néel model, used to describe non-interacting systems, whereas the EuS nanocrystals can only be described in the framework of strongly interacting/spin-glass-like systems.

Experimental methods

Chemicals

Water was purified using a Sation 8000/Sation 9000 purification unit. Styrene (Aldrich 99%) was purified over a column of neutral Al_2O_3 and stored at 4 °C, under N_2. All the other reagents: α,α'- azobis(isobutyronitrile) (AIBN, Fluka >98%), dodecyl sulfate sodium salt (SDS, Aldrich), potassium persulfate (KPS, Panreac 98%), hexadecane (HD, Aldrich 99%), oleylamine (OA, Aldrich 70%), $EuCl_3 \cdot 6H_2O$ (Aldrich 99.9%), 1,10-phenanthroline (phen, Aldrich 99%), sodium diethyldithiocarbamate monohydrate (Nadtc, Aldrich), isopropanol (Labscan) and methanol (Aldrich) were used as purchased.

Synthesis of EuS nanocrystals

EuS nanocrystals were synthesized using the lyothermal decomposition of Eu(III) diethyldithiocarbamato complexes as described elsewhere.[4–7] First, the heteroligand europium(III) complex $\{Eu[S_2CN(C_2H_5)_2]_3(C_{12}H_8N_2)\}$: [Eu(dtc)$_3$(phen)] (dtc: diethyldithiocarbamate; phen: phenanthroline), was synthesized according to literature methods.[4,30] Typically, 20 ml of a 0.5 mol dm^{-3} aqueous solution of phenanthroline hydrate was mixed with 20 ml of an aqueous solution of $EuCl_3 \cdot 6H_2O$ (0.5 mol dm^{-3}), under vigorous stirring. To this mixture, 20 ml of a 1.5 mol dm^{-3} aqueous solution of Nadtc$\cdot H_2O$ was added drop-wise resulting in an orange precipitate (yield: 85%). This solid was filtered, washed with distilled water and then dried in a desiccator. The compound was characterized by microanalysis and vibrational spectroscopy:

[Eu(dtc)$_3$(phen)], elemental analysis (%): found C, 40.65; H, 4.91; N, 8.64; calculated C, 41.74; H, 4.93; N, 9.01. IR and (Raman) major bands (υ/cm^{-1}): 2975 (2977) [υ(C–H)], 1482 (1483) [υ(C–N)], 1000 (994.3) [υ(C–S)] for the dithiocarbamato ligand; 1623 (1624) and 1604 (1602) skeleton vibration of the benzene ring, 852 (843.5) and 730 (720.2) [υ(C–CH)].

The synthesis of EuS nanocrystals was then performed by injecting an oleylamine solution of [Eu(dtc)$_3$(phen)] into hot OA, under a N_2 flow. In a typical synthesis, 3 ml of OA was first heated up to 315 °C. In the meantime, a mixture of the precursor (0.25 mmol) in 2 ml of OA was prepared and then injected into the hot OA, the reaction continued at 315 °C over 1 h. The deep purple product was cooled to room temperature and treated with a mixture of isopropanol : methanol (3 : 1) yielding a powder consisting on EuS nanospheres capped with OA molecules. The powders were easily dispersed in non-polar solvents, such as hexane and toluene, due to OA molecules coordinated at the nanocrystals' surfaces. To alter the morphology of the particles from spherical to cubic nanoparticles, the solution of oleylamine containing the precursor was heated rapidly to 315 °C, over 1 h.

In situ synthesis of EuS/poly(styrene) nanocomposites

For the *in situ* polymerizations in a miniemulsion, the procedure was as follows: typically (for a 25 mL batch) the monomer (0.032 mol) was first mixed with the hydrophobe HD (0.331 mmol), AIBN (0.128 mmol) and the oleylamine capped EuS nanocrystals. Separately, an aqueous solution of sodium dodecyl sulfate (SDS, 0.200 mmol) containing $NaHCO_3$ (0.173 mmol) was prepared. The organic phase was then added to this aqueous solution and left under vigorous magnetic stirring over 30 min. After this period the mixture was sonicated (amplitude 80%, 20 W power, Sonics-Vibracel Sonifier) for 7 min. The stable miniemulsion obtained was transferred to a conventional "jacket" glass reactor (30 mL capacity), equipped with a thermostat bath, condenser, mechanical stirrer, and nitrogen inlet. The reactor content was deoxygenated by purging with N_2 for 20 min with the temperature set at 70 ± 1 °C. When KPS was used as the initiator, it was added to the reaction mixture at this point. The reaction took place over 4 h under mechanical stirring at 500 rpm. Monomer conversion was determined gravimetrically and values typically around 80% were obtained when AIBN was used as the precursor. This latex consists of a mixture of free PS particles and EuS/PS, which could be then enriched in the nanocomposite by successive centrifugation procedures (4000 rpm). The final samples were then kept under N_2 for further characterization. The formation of PS after polymerization was confirmed by FT-IR spectroscopy and the presence of EuS was assessed by powder XRD (ESI†). For GPC analysis, the nanocomposite was separated from free poly(styrene) and dissolved in DMF with a concentration of 10 mg mL^{-1}.

Instrumentation

Spectroscopic techniques. A Jasco V 560 UV/VIS spectrophotometer was used for the UV/VIS absorption and reflectance spectra using respectively the solvent and MgO powder as references. The FT infrared spectra were recorded using a Matson 700 FT-IR Spectrometer and dry KBr disks. The europium content in the nanocomposite was measured by ICP using a Jobin Yvon instrument (Analytical Laboratories, University of Aveiro).

Diffraction and electron microscopic techniques. X-Ray powder diffraction (XRD) was performed on samples deposited on silicon substrates, using a Philips X'Pert instrument operating with Cu Kα radiation (λ = 1.54178 Å) at 40 kV/50 mA. Transmission electron microscopy (TEM), energy dispersion spectroscopy (EDS) and electron diffraction were carried out on a Hitachi H-9000 microscope operating at 300 kV or using a JEOL 2010 transmission electron microscope, both operating at 200 kV. To prepare the TEM samples, a drop of the colloid was deposited on the carbon-coated copper grids and the solvent was left to evaporate.

Magnetic measurements. The magnetic AC susceptibility was recorded at increasing temperatures (up to 30 K) and selected frequencies in the 1–1488 Hz range, after an initial cooling from RT down to 2 K in the absence of the field (ZFC procedure). The magnetic DC susceptibility was recorded at increasing temperatures (up to 100 K) after an initial cooling from RT down to 2 K under a ZFC procedure, and after cooling from 100 K down to 2 K at the measuring field (50 Oe—FC procedure). Magnetization was recorded as a function of magnetic field (from −50 kOe up to +50 kOe), at selected temperatures between 2 and 30 K. Measurements were performed on a SQUID magnetometer (model MPMS-XL) at Universidad de Zaragoza.

Chromatographic techniques. Gel permeation chromatography (GPC) was performed with DMF as the mobile phase at 35 °C, a Waters 510 pump set to a flow rate of 1 mL min^{-1}, three Styragel columns (Polymer Standard Service, pore sizes 1×10^5, 1×10^3, and 1×10^2), and a Waters 2410 refractive index detector. Molecular weights were determined using PSS software with a calibration based on linear polystyrene standards (range 1–2000 k, PDI < 1.07).

Conclusions

In summary, we have synthesized oleylamine capped EuS nanocrystals and investigated their use as nanoscopic fillers for

polymer based composites. Although the magnetic properties of EuS nanocrystals have been reported elsewhere[6,7] this is the first study of an *in situ* prepared polymer composite based on such a nanomaterial. In using this synthetic strategy, we succeeded in obtaining a EuS/poly(styrene) nanocomposite whose magnetic properties are distinct from the starting EuS nanocrystals as a result of their efficient dispersion within the polymer beads. As a consequence, the magnetic behaviour of EuS nanocrystals embedded in the PS beads are well described by the super-paramagnetic Néel model, used to describe non-interacting systems, whereas the starting EuS nanocrystals can only be described in the framework of strongly interacting/spin-glass-like systems.

Further studies on the magnetic behaviour of EuS nanocrystals dispersed in a range of polymer matrices, including blends of these materials, will enable other questions to be answered. For example, our preliminary magnetic measurements of EuS/PS blends show a distinct behaviour from the EuS nanocrystals and EuS/PS composites prepared by miniemulsion polymerization. Thus these results strongly advise consideration of the chemical route employed for the nanocomposites preparation when studying the magnetism of EuS nanocrystals in polymers.

Acknowledgements

A. S. Pereira thanks Fundação para a Ciência e Tecnologia (FCT) for a PhD grant. N.J.O. Silva acknowledges CSIC for a I3P contract. This work was funded by FCT and FEDER (project PTDC/QUI/67712/2006). The work in Zaragoza has been supported by the research grants MAT2007–61621 and CSD2007–00010 from the Ministry of Education. We thank Dr A. Lopes (U. Aveiro) for some of the TEM analysis.

References

1 See, for example: (*a*) *The Chemistry of Nanomaterials*, ed. C. N. R. Rao, A. Müller and A. K. Cheetham, Wiley-VCH, Weinheim, 2003; (*b*) *Nanoparticles*, ed. G. Schmid, Wiley-VCH, Weinheim, 2004; (*c*) G. A. Ozin and A. C. Arsenault, in *Nanochemistry*, RSC, Cambridge, 2005; (*d*) *Nanoscale Materials*, ed. L. M. Liz-Marzán and P. V. Kamat, Kluwer Academic Publishers, Dordrecht, 2003; (*e*) A. Eychmüller, *J. Phys. Chem. B*, 2000, **104**, 6514; (*f*) M. Remskar, *Adv. Mater.*, 2004, **16**, 1497; (*g*) E. Roduner, *Chem. Soc. Rev.*, 2006, **35**, 583; (*h*) S. Kumar and T. Nann, *Small*, 2006, **2**, 316; (*i*) S. Eustis and M. A. El-Sayed, *Chem. Soc. Rev.*, 2006, **35**, 209.
2 (*a*) C. B. Murray, D. J. Norris and M. G. Bawendi, *J. Am. Chem. Soc.*, 1993, **115**, 8706; (*b*) B. M. Tissue, *Chem. Mater.*, 1998, **10**, 2837; (*c*) A. C. C. Esteves and T. Trindade, *Curr. Opin. Solid State Mater. Sci.*, 2002, **6**, 347; (*d*) S. B. Sinnott, *J. Nanosci. Nanotechnol.*, 2002, **2**, 113; (*e*) I. W. Hamley, *Nanotechnology*, 2003, **14**, R39; (*f*) J. Park, K. An, Y. Hwang, J. Park, H. Noh, J. Kim, J. Park, N. Wang and T. Hyeon, *Nat. Mater.*, 2004, **3**, 891; (*g*) O. Masala and R. Seshadri, *Annu. Rev. Mater. Res.*, 2004, **34**, 41; (*h*) D. Chen, G. Wang and J. Li, *J. Phys. Chem. C*, 2007, **111**, 2351; (*i*) N. Pinna, *J. Mater. Chem.*, 2007, **17**, 2769.
3 (*a*) T. Trindade and P. O'Brien, *Adv. Mater.*, 1996, **8**, 161; (*b*) T. Trindade, P. O'Brien, X.-M. Zhang and M. Motevalli, *J. Mater. Chem.*, 1997, **7**, 1011; (*c*) F. V. Mikulec, M. Kuno, M. Bennati, D. A. Hall, R. G. Griffin and M. G. Bawendi, *J. Am. Chem. Soc.*, 2000, **122**, 2532; (*d*) O. C. Monteiro, A. C. C. Esteves and T. Trindade, *Chem. Mater.*, 2002, **14**, 2900; (*e*) S. L. Cumberland, K. M. Hanif, A. Javier, G. A. Khitrov, G. F. Strouse, S. M. Woessner and C. S. Yun, *Chem. Mater.*, 2002, **14**, 1576; (*f*) W. P. Lim, Z. Zhang, H. Y. Low and W. S. Chin, *Angew. Chem., Int. Ed.*, 2004, **43**, 5685; (*g*) Y. Li, M. Afzaal and P. O'Brien, *J. Mater. Chem.*, 2006, **16**, 2175.
4 M. D. Regulacio, N. Tomson and S. L. Stoll, *Chem. Mater.*, 2005, **17**, 3114.
5 T. Mirkovic, M. A. Hines, P. S. Nair and G. D. Scholes, *Chem. Mater.*, 2005, **17**, 3451.
6 F. Zhao, H. L. Sun, S. Gao and G. Su, *J. Mater. Chem.*, 2005, **15**, 4209.
7 F. Zhao, H. L. Sun, G. Su and S. Gao, *Small*, 2006, **2**, 244.
8 T. R. McGuire and M. W. Shafer, *J. Appl. Phys.*, 1964, **35**, 984.
9 W. J. Nolting, *J. Phys. C: Solid State Phys.*, 1982, **15**, 733.
10 W. Chen, X. Zhang and Y. Huang, *Appl. Phys. Lett.*, 2000, **76**, 2328.
11 I. N. Goncharenko and I. Mirebeau, *Phys. Rev. Lett.*, 1998, **80**, 1082.
12 W. Chen, X. Zhang and Y. Huang, *Appl. Phys. Lett.*, 2000, **76**, 2328.
13 K. Tanaka, N. Tatehara, K. Fujita and K. Hirao, *J. Appl. Phys.*, 2001, **89**, 2213.
14 S. C. Farmer and T. E. Patten, *Chem. Mater.*, 2001, **13**, 3920.
15 S. Y. Lu, M. L. Wu and H. L. Chen, *J. Appl. Phys.*, 2003, **93**, 5789.
16 C. Barthet, A. J. Hickey, D. B. Cairns and S. P. Armes, *Adv. Mater.*, 1999, **11**, 408.
17 P. Tangboriboonrat and U. Buranabunya, *Colloid Polym. Sci.*, 2001, **279**, 615.
18 F. Caruso, H. Lichtenfeld, E. Donath and H. Mohwald, *Macromolecules*, 1999, **32**, 2317.
19 (*a*) K. Landfester, F. Tiarks, H. Hentze and M. Antonietti, *Macromol. Chem. Phys.*, 2000, **201**, 1; (*b*) J. Pyun and K. Matyjaszewski, *Chem. Mater.*, 2001, **13**, 3436; (*c*) G. Kickelbick, *Prog. Polym. Sci.*, 2003, **28**, 83; (*d*) E. Bourgeat-Lami, M. Insulaire, S. Reculusa, A. Perro, S. Ravaine and E. Duguet, *J. Nanosci. Nanotechnol.*, 2006, **6**, 432; (*e*) Y. Lu, Y. Mei, M. Schrinner, M. Ballauff, M. W. Moller and J. Breu, *J. Phys. Chem. C*, 2007, **111**, 7676; (*f*) A. C. C. Esteves, L. Bombalski, T. Trindade, K. Matyjaszewski and A. Barros-Timmons, *Small*, 2007, **3**, 1230.
20 (*a*) K. Landfester, *Adv. Mater.*, 2001, **13**, 765; (*b*) F. Tiarks, K. Landfester and M. Antonietti, *Langmuir*, 2001, **17**, 5775; (*c*) A. C. C. Esteves, A. Barros-Timmons, T. Monteiro and T. Trindade, *J. Nanosci. Nanotechnol.*, 2005, **5**, 766; (*d*) N. Joumaa, M. Lansalot, A. Théretz, A. Elaissari, A. Sukhanova, M. Artemyev, I. Nabiev and J. H. M. Cohen, *Langmuir*, 2006, **22**, 1810; (*e*) M. L. P. Ha, B. P. Grady, G. Lolli, D. E. Resasco and W. T. Ford, *Macromol. Chem. Phys.*, 2007, **208**, 446; (*f*) M. A. Martins, M. C. Neves, A. C. C. Esteves, P. I. Girginova, A. J. Guiomar, V. S. Amaral and T. Trindade, *Nanotechnology*, 2007, **18**, 215609.
21 N. R. Jana, *Angew. Chem., Int. Ed.*, 2004, **43**, 1536.
22 J. Yang, J. Zeng, S. Yu, L. Yang, G. Zhou and Y. Qian, *Chem. Mater.*, 2000, **12**, 3259.
23 J. L. Dormann, D. Fiorani and E. Tronc, *Adv. Chem. Phys.*, 1997, **98**, 285.
24 N. J. O. Silva and V. S. Amaral, *Appl. Phys. Lett.*, 2008, **92**, 026102.
25 M. L. Redígolo, D. S. Koktysh, S. J. Rosenthal, J. H. Dickerson, Z. Gai, L. Gao and J. Shen, *Appl. Phys. Lett.*, 2006, **89**, 222501.
26 J. L. Dormann, D. Fiorani, R. Cherkaoui, E. Tronc, F. Lucari, F. D'Orazio, L. Spinu, M. Noguès, H. Kachkachi and J. P. Jolivet, *J. Magn. Magn. Mater.*, 1999, **203**, 23.
27 S. Thongchant, Y. Hasegawa, Y. Wada and S. Yanagida, *J. Phys. Chem. B*, 2003, **107**, 2193.
28 L. C. R. Néel, *C. R. Hebd. Seances Acad. Sci.*, 1949, **228**, 664.
29 J. L. Dormann, F. D'Orazio, F. Lucari, E. Tronc, P. Prene, J. P. Jolivet, D. Fiorani, R. Cherkaoui and M. Noguès, *Phys. Rev. B*, 1996, **53**, 14291.
30 R. A. Ivanov, I. E. Korsakov, N. Kuzmina and A. R. Kaul, *Mendeleev Commun.*, 2000, **2**, 83.

